Research Article Vol. 3, No. 7 / July 2016 / Optica 718

Invisibility exposed: physical bounds on passive cloaking

FRANCESCO MONTICONE AND ANDREA ALÙ*

Department of Electrical and Computer Engineering, The University of Texas at Austin, Austin, Texas 78712, USA
**Corresponding author: alu@mail.utexas.edu*

Received 11 January 2016; accepted 23 May 2016 (Doc. ID 264125); published 5 July 2016

Invisibility cloaks have been one of the major breakthroughs in the field of metamaterials, and several techniques are currently available to suppress the electromagnetic scattering from different objects. So far, however, theoretical and experimental results have consistently shown fundamental challenges in terms of the bandwidth and size of the object to be hidden. Understanding the bandwidth limitations of cloaking therefore becomes important to assess the applicability and potential of cloaking devices in practical scenarios. While it is generally accepted that cloaking is difficult to achieve, no work to date has quantified this issue for general invisibility devices. Here, by applying the Bode–Fano theory of broadband matching, we derive fundamental bounds on bandwidth and performance for general passive cloaking schemes applied to planar objects, determined by the properties of the object to be hidden, and then explore their implications in three-dimensional scenarios. Our results define a general framework to estimate the ultimate performance of passive cloaks and suggest that fundamentally new directions, involving nonlinearities and active metamaterials, become necessary to realize broadband cloaking, opening a new phase in the quest for invisibility.

OCIS codes: (230.3205) Invisibility cloaks; (290.0290) Scattering; (290.5839) Scattering, invisibility; (160.3918) Metamaterials.

http://dx.doi.org/10.1364/OPTICA.3.000718

1. INTRODUCTION

The idea of invisibility has inspired the human imagination for centuries. However, a systematic scientific treatment of the problem of invisibility has become possible only in recent times. In particular, the advent of metamaterials [1] at the beginning of the 21st century enabled fundamental steps forward in the quest for invisibility, with the design and fabrication of the first proof-of-concept examples of "invisibility cloaks." After a decade of extensive research efforts, several techniques are now available to achieve this goal, the most popular arguably being transformation optics [2,3] and scattering-cancellation cloaking [4,5], among a few others [6]. In general, passive cloaks have been successfully designed to drastically suppress the scattering of a given object in a narrow frequency window, hence making the cloaked object undetectable to quasi-monochromatic signals. However, the theoretical, numerical, and experimental investigations carried out in this area during the past few years have highlighted major challenges associated with achieving invisibility over broader frequency bandwidths, especially for large objects [7–11], an issue that appears to stem from fundamental causality and passivity limitations, independent of the employed cloaking technique. A few papers have recently proposed interesting attempts to derive bandwidth limitations for cloaking [12–15], but these approaches are restricted to specific cloaking techniques, making the bounds not generally applicable. Here, we aim at deriving physical bounds on the cloaking bandwidth and performance, valid for any linear, causal, and passive cloaking device, showing that these limitations are uniquely imposed by the characteristics of the object to be cloaked and the central wavelength of excitation.

When a broadband beam of light (a short light pulse, or incoherent white light) encounters an obstacle along its path, such as a particle, an ensemble of particles, or a slab, the various spectral components undergo scattering and reflections, inevitably attenuating and distorting the transmitted light beam [Figs. 1(a) and 1(b)]. The goal of a cloaking device is to prevent an impinging light beam from suffering any such distortion when it encounters an obstacle. In order to make a lossless object invisible, the cloak has to restore the impinging field distribution (in amplitude and phase) all around the cloaked object by suppressing its total scattering cross section (SCS). We stress that this is different, and significantly more challenging, than giving the impression of transparency using an optical system that allows replicating the amplitude distribution of the incident field for specific excitation conditions, as in [16–18] and other camouflaging systems.

All cloaking devices designed so far have achieved this goal over narrow bandwidths, while the cloak performance rapidly deteriorates away from the central frequency, even leading to largely enhanced scattering in nearby regions of the spectrum. Figure 1(c), for instance, shows the typical dispersion of popular cloaking schemes applied to an impenetrable sphere, implying a scattering response sketched in Fig. 1(d), with reduced scattering for one

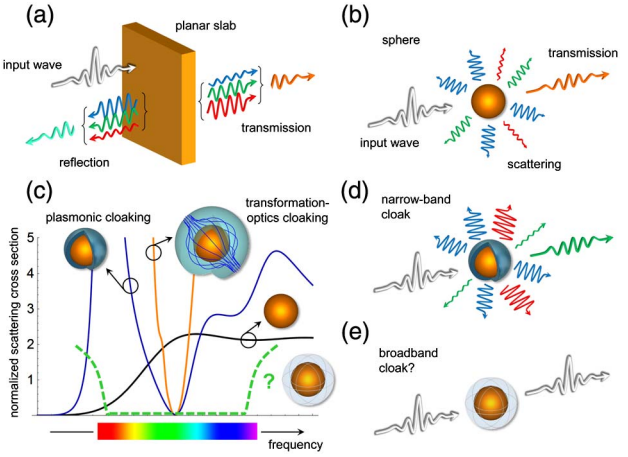

Fig. 1. Issues with broadband cloaking. (a), (b) A broadband light beam is reflected/scattered by an obstacle (a dielectric slab or a sphere), leading to distorted transmission. (c) Scattering performance of typical cloaking devices (blue, plasmonic cloaking [4]; orange, transformation-optics cloaking [3]) applied to an impenetrable spherical object (black) (details in Supplement 1). (d) Under broadband illumination, e.g., containing all the wavelengths/colors of the visible spectrum, a narrow-band cloak has typically the effect of simply "redistributing" the scattering among the different wavelengths, e.g., making the object invisible for a certain color, while largely increasing the scattering for other colors. (e) The proposed cloaking bounds allow determining whether broadband cloaking—for example, encompassing the entire visible range [green dashed curve in (c)]—is possible.

wavelength but enhanced scattering for neighboring ones. This fact is associated to recently derived global bounds on cloaking [19,20], which show that invisibility in a given frequency window can be achieved only at the expense of higher scattering in other regions of the frequency spectrum. Although such global bounds do not forbid the possibility of broadband invisibility, we show in the following that there are more stringent local bounds that cannot be overcome by passive cloaks of arbitrary complexity. In the following, our ultimate goal is to assess, for a given scatterer, the available continuous cloaking bandwidth and total scattering reduction. For example, would it be possible to realize robust scattering reduction over a broad wavelength range, or for short impinging pulses, as sketched in Fig. 1(e), or even over the entire visible range for human-scale objects?

2. RESULTS

A. Cloaking of Planar Objects

The microwave circuit community has dealt with a somewhat related problem in the context of impedance-matching filter theory. In many practical scenarios, a generic load, such as an antenna, an amplifier, or an entire subcircuit, is accompanied by a suitably designed matching network, aimed at reducing its reflections and ensuring proper power delivery. In this context, Bode–Fano theory [21,22,23] was developed to derive general theoretical limitations on the bandwidth over which a given load may be matched. Interestingly, this theory shows that stringent bounds on the bandwidth over which the local reflection coefficient Γ can be minimized are imposed by the reactive properties of the load itself, under the general assumptions of a linear, causal, and passive (lossless) matching network. Considering the analogies between the problems of impedance matching and of cloaking—and the fact that a polarizable material, in essence, is characterized by a local reactance for the applied field—the Bode–Fano approach is particularly appealing for our purposes. As a first step in this direction, we start by analyzing a one-dimensional (1D) cloaking problem, namely, the problem of making a dielectric slab invisible to an incident plane wave [Fig. 2(a)] by suppressing its reflection. As shown in Fig. 2(b) (black line), the reflection coefficient of the slab is characterized by a periodic alternation of peaks and zeros, arising from the interference between multiple reflections at the two dielectric–air interfaces, and each zero corresponds to a conventional Fabry–Perot resonance of the slab. As shown in Supplement 1, this frequency response is well approximated in the neighborhood of any zero by the response of a lumped-element shunt resonator composed of a capacitor $C = d\epsilon_0(\epsilon - 1)/2$ in parallel with an inductor $L = 2d\epsilon\mu_0/m^2\pi^2(\epsilon - 1)$, where ϵ_0 and μ_0 are the free-space permittivity and permeability, respectively, d is the slab thickness, ϵ is its relative permittivity, and m is the order of the considered Fabry–Perot resonance. By also modeling the semi-infinite free-space region behind the slab as a resistor $R = \eta_0 = \sqrt{\epsilon_0/\mu_0}$, we are able to locally convert, within a certain frequency window of interest, the dynamic scattering problem into a lumped circuit problem (red line), as shown in Figs. 2(b) and 2(c). This equivalent problem can now be handled by Bode–Fano theory, with

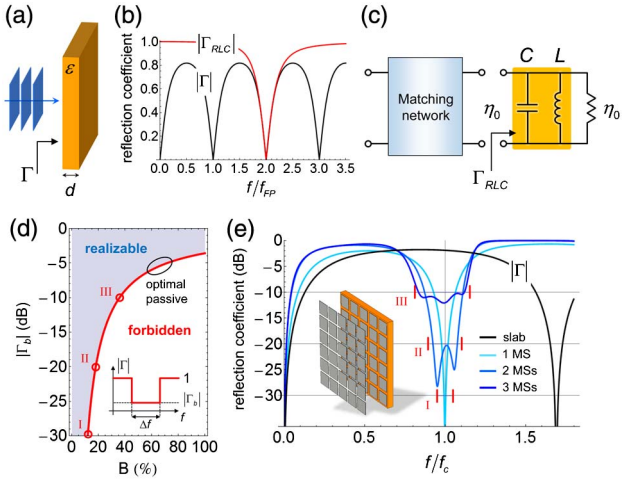

Fig. 2. Physical bounds on 1D cloaking. (a), (b) Dielectric slab normally illuminated by a plane wave and amplitude of its reflection coefficient Γ (black curve), as a function of frequency (normalized to the frequency of its first Fabry–Perot resonance f_{FP}). Relative permittivity of the slab is $\epsilon = 10$. (c) Equivalent lumped-element circuit that locally models the slab response in the neighborhood of a Fabry–Perot resonance [red curve in (b)]. A generic passive cloak in front of the slab is represented by a reactive matching network aimed at reducing the reflection around the frequency of interest f_c. (d) Physical bound on the cloaking performance, in terms of fractional cloaking bandwidth $B = \Delta f/f_c$ and in-band reflection coefficient $|\Gamma_b|$, for a slab with $\epsilon = 10$ and thickness $d = \lambda_c/10$ at the cloaking wavelength λ_c. The thick red line indicates the performance of the optimal passive cloak. (e) Examples of planar mantle cloaks applied to the slab considered in (d), showing how they perform in relation to the physical bound at three different levels of reflection, as indicated by the red line segments [corresponding to the red circles in (d)]. The mantle cloaks are made of stacked metasurfaces, as shown in the inset, with optimized reactance and separation (details in Supplement 1).

the goal of finding bandwidth limitations on the reflection reduction. Using circuit-theory terminology, the "load" to be matched is the scatterer (the planar slab) in parallel with the entire semi-infinite space behind it, compactly modeled by the RLC resonator in Fig. 2(c), while the matching network represents an arbitrary passive and lossless structure in front of the slab aimed at reducing its reflection (i.e., an invisibility cloak). It is important to stress that the equivalent circuit load is determined by the intrinsic properties of the scattering system under consideration in the frequency window of interest, which do not change when a cloak is applied in front of the slab. It is clear that, if we had the option of altering the obstacle itself (e.g., by modifying its composition, or cutting through the object, as in [24]) or the background medium (e.g., by making it diffusive, as in [25], or by introducing a ground plane, as in carpet cloaking [26]), the cloaking problem would become much simpler. Here, on the contrary, we ask whether there are fundamental bandwidth restrictions on the operation of an arbitrary passive, linear cloak applied to the object of interest in free space.

As detailed in Supplement 1, the application of Bode–Fano theory to the scattering load in Fig. 2(c) produces a physical bound on the local cloaking performance. This takes the form of an inequality on the product of the fractional cloaking bandwidth $B = \Delta f/f_c$ and the natural logarithm of the in-band reflection coefficient Γ_b:

$$B \ln\left(\frac{1}{|\Gamma_b|}\right) \leq \frac{c_0}{d(\epsilon - 1)f_c}, \tag{1}$$

which is valid in the neighborhood of any Fabry–Perot resonance (c_0 is the speed of light in the surrounding medium). Notably, the bound depends uniquely on the central frequency of excitation f_c, and on the properties of the dielectric slab and the background medium around this frequency, without any assumption on the cloak or cloaking methodology, other than its passivity, linearity, and causal response. Inequality (1) is visualized in Fig. 2(d) for an example with $\epsilon = 10$ and thickness $d = \lambda_c/10$ at the cloaking wavelength λ_c. The thick red line represents the optimal tradeoff between the cloaking bandwidth and the in-band reflection coefficient, and it marks the separation between realizable and unfeasible cloaking performance. The forbidden region can never be reached, independent of the cloak complexity. The derived bound becomes less applicable for larger bandwidths, since it is based on modeling the periodic response in Fig. 2(a) (black line) with its local circuit-based approximation (red line), but it is very accurate for larger scattering suppressions, for which the bandwidth narrows down (if of interest, the bound may be improved by considering higher-order circuit models that fit the dynamic response of the slab over a broader frequency range). Most importantly, it follows directly from Eq. (1) that ideal cloaking, with zero reflection, can only be achieved over a zero-measure bandwidth, and Eq. (1) provides a direct way to quantify the required tradeoff between cloaking bandwidth and overall reflection suppression for imperfect cloaking.

To better understand the effect of these limitations, consider a planar mantle cloak made of an ultra-thin metasurface tailored to suppress the reflections from the slab of Fig. 2. The cloak acts as a shunt impedance that, if properly tailored to compensate the slab reactance, brings the reflection coefficient to zero at the desired frequency [light blue curve in Fig. 2(e)]. While this simple cloak is able to achieve perfect transparency at a single frequency, its bandwidth is far from the optimum, given by Eq. (1), for different levels of in-band reflection, as seen in Figs. 2(d) and 2(e). In order to widen the cloak bandwidth, we may increase the number of metasurfaces in front of the slab, analogous to what is routinely done in broadband microwave filters when multiple matching stages are used to broaden the frequency response [27]. By stacking more metasurfaces, and optimizing their impedance and separation, the cloak bandwidth can indeed be increased, approaching the physical bound for a desired level of reflection, as shown in Figs. 2(d) and 2(e) for two and three metasurfaces (darker blue curves). Details on the designs of the different mantle cloaks in Fig. 2(e) are provided in Supplement 1. We have verified that, as the number of layers is further increased, the response slowly locally converges to the ultimate bound in Eq. (1). In the optimized multi-layered designs, the reflection coefficient in Fig. 2(e) does not go to zero at the central frequency any longer, but it rather shows in-band ripples and a steeper response at the edges, which guarantees a better utilization of the considered bandwidth, as in conventional Chebyshev filters [27]. Following our theory, an optimally broadband passive cloak should not aim at realizing large scattering reduction at specific frequencies, but it should carefully distribute the available scattering suppression, determined by Eq. (1), over the allowed bandwidth B to keep it at the acceptable level $|\Gamma_b|$ [inset of Fig. 2(d)]. Values of in-band scattering below $|\Gamma_b|$ actually play a detrimental role in terms of bandwidth.

B. Cloaking of Three-Dimensional Objects

Having established stringent local bounds, independent of the specific cloaking technique, on the bandwidth and reflection suppression in this 1D problem, we now propose to extend the above considerations to three-dimensional (3D) objects. From a physical standpoint, planar reflection and spherical scattering are related phenomena, as they both arise from the same microscopic mechanism, namely, the reradiation of the extinguished power by polarization or conduction currents induced on a material body. A relevant difference due to geometry is the fact that, while in the 1D case a plane wave impinging on a transversely homogenous obstacle (e.g., a slab) is scattered into a single scattering channel, corresponding to specular reflection, in the 3D scenario the incident plane wave can be scattered by the obstacle (e.g., a sphere) into an infinite discrete set of channels, associated with the orthogonal spherical modes radiating in free space, i.e., spherical waves with different angular momentum. Cloaking aims at minimizing the total scattered power by suppressing the coupling to all these channels, so that the input propagating wave does not lose any energy interacting with the object. More specifically, here we define cloaking as the ability to suppress the total SCS of a given object. We also would like to stress that this definition, and therefore our bounds, do not imply that the original object needs to be shielded inside an impenetrable box (i.e., the incident wave is allowed to propagate through the concealed object if the object is penetrable). However, if one is interested in deriving cloaking bounds independent of the nature of the object to be hidden, it is possible to apply our bounds considering as a cloaked object an impenetrable perfectly conducting surface surrounding the region of interest.

In the relevant case of spherically symmetric scatterers [Fig. 3(a)]—a typical benchmark for cloaking devices—angular momentum is conserved, which allows treating each scattering

channel independently, but the following discussion can also be extended to the case of coupled harmonics in the most general scenario. The coupling coefficients to the different scattering channels, or scattering coefficients, can be obtained analytically by applying Mie theory [28] and can be conveniently written as $c_n = -(1 + iV_n/U_n)^{-1}$ for the nth spherical harmonic, where the quantities U_n and V_n (real in the lossless case) are obtained by imposing proper electromagnetic boundary conditions on each spherical interface after expanding the incident plane wave as a discrete sum of spherical harmonics (Supplement 1 and Ref. [28]). As an example, Fig. 3(b) shows the first transverse-magnetic (TM) and transverse-electric (TE) scattering coefficients of an impenetrable perfectly conducting sphere as a function of frequency, showing an alternation of peaks (scattering resonances, $V_n = 0$) and zeros ($U_n = 0$) that reveals a qualitative resemblance to the reflection coefficient Γ of a dielectric slab [Fig. 2(b)]. However, these scattering coefficients do not represent spherical reflections in the conventional sense, since in the 3D scenario we deal with spherical harmonics, for which the coordinate system ends at the origin (all the incident energy associated with a given spherical harmonic "bounces back" from the origin, and therefore spherical reflection always has unitary amplitude). Nevertheless, as more extensively discussed in Supplement 1, we propose to locally model a given scattering coefficient as the reflection coefficient of an equivalent causal circuit, as indicated in Fig. 3(c), locally following the same constraints on dispersion. We shall see in the following that, when the overall scattering is considered, this assumption leads to meaningful bounds, which agree well with other heuristic cloaking limitations derived from different

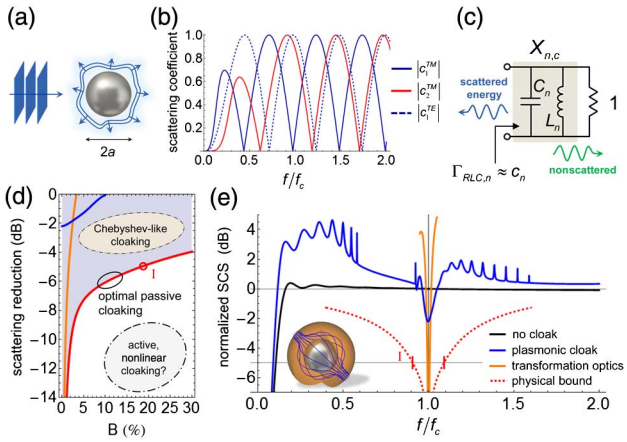

Fig. 3. Physical bounds on 3D cloaking. (a) Spherical scatterer illuminated by a plane wave. The scattering wavefront results from the superposition of multiple spherical harmonics. (b) Amplitude of the first three scattering coefficients, for an impenetrable sphere of radius $a = \lambda_c$ at the wavelength of interest. (c) Equivalent circuit for the nth scattering coefficient. The reflection coefficient $\Gamma_{\mathrm{RLC},n}$ of the circuit locally approximates the scattering coefficient c_n, while the nonscattered energy dissipates on the unitary resistor. (d) Physical bound on the cloaking performance, in terms of fractional bandwidth $B = \Delta f/f_c$ and in-band scattering reduction, for the sphere considered in (b). The thick red line indicates the performance of the optimal passive cloak. The performance of a typical transformation-optics cloak (orange curve) and a plasmonic cloak (blue) is also plotted (details in Supplement 1). (e) Normalized scattering cross section (SCS) of the uncloaked object (black curve) and of the two cloaking devices considered in (d), compared to the physical bound (dashed red line).

considerations. In particular, for a lossless scatterer the circuit is composed of a scattering reactance $X_n = V_n/2U_n$, which models the scatterer geometry and its reactive near field for a given order n, connected in parallel with a unitary resistor that represents the surrounding environment, independent of the scatterer, analogous to the equivalent circuit of the dielectric slab in Fig. 2(c). It can be verified that the reflection coefficient of such a circuit is indeed equal to the scattering coefficient c_n, while the resistor fulfills power conservation by dissipating the portion of input energy that is not scattered. After further enforcing passivity by suitably modifying the scattering reactance, as detailed in Supplement 1, we locally approximate this reactive part with a lumped inductor-capacitor resonator [Fig. 3(c)] having the same response in the frequency neighborhood of interest. We would like to stress that an RLC equivalent circuit, which isolates an individual pole-zero of the system, is sufficient to estimate the bounds for most, if not all, cloaking systems proposed to date. This is due to the fact that the operational bandwidth of cloaking devices is typically narrow, and it is dominated by a single resonance. Our technique can also be extended to the case of multiple resonances, but the accuracy improvement of the derived bounds would be minimal. In general, the derivation of lumped-element equivalent circuits is currently an important topic in different areas of optics (see, e.g., [29,30]), as it allows modularizing the optical response and translating relevant concepts and methods from circuit and network theory to the optical domain.

Similar to the 1D case considered above, by applying Bode–Fano theory to the local RLC network, we obtain a bound on the suppression bandwidth of the circuit reflection coefficient, i.e., the causal local approximation of the nth scattering coefficient. An overall bound on the total SCS of an object can then be obtained by properly summing the individual bounds for each harmonic (Supplement 1). After some manipulation, we find that, for a given cloaking bandwidth Δf around the central frequency f_c, the in-band SCS is fundamentally constrained by

$$\mathrm{SCS} \geq \frac{\lambda_c^2}{2\pi}\sum_{n=1}^{N}(2n+1)\left[\exp\left(\frac{-1/\Delta f}{\max[C_{n,\pm}^{\mathrm{TM}}]}\right) + \exp\left(\frac{-1/\Delta f}{\max[C_{n,\pm}^{\mathrm{TE}}]}\right)\right], \tag{2}$$

where N is the number of non-negligible scattering coefficients, which is typically of the same order as $k_0 a$, where k_0 is the free-space wavenumber and a is the radius of the spherical scatterer [28]. For each TE and TM spherical harmonic, the bound is directly related to the properties of the object to be cloaked through the quantity

$$C_{n,\pm} = \left[\frac{\mathrm{d}Y_n(\omega)}{\mathrm{d}\omega} \pm \frac{Y_n(\omega)}{\omega}\right]_{\omega=\omega_c}, \tag{3}$$

where $Y_n = 1/(X_{n,c})$, and $X_{n,c}$ is the modified passive scattering reactance (Supplement 1). The sign in Eq. (3) is chosen to give the most stringent bound at the angular frequency ω_c of interest, corresponding to the operation of taking the maximum in the denominators in Eq. (2). Given an arbitrary object to be cloaked, the multipolar contributions to its SCS can be calculated analytically (e.g., with Mie theory) or numerically in a neighborhood of the cloaking frequency ω_c, and these quantities can then be used to derive the scattering reactances in Eq. (3) that determine the bounds.

In the presented theory, we assume that the effect of a cloak can be locally represented by adding a reactive matching network in front of the scattering loads in Fig. 3(c), without changing the original RLC circuit (the reactive part of the load is an intrinsic property of the original uncloaked scatterer, as the LC resonator captures the locally resonant nature of that object). In other words, within our local approximation, we expect that a passive and causal cloak has essentially the effect of changing the local value of the scattering coefficient and of its first derivative, an effect that can be fully represented by a reactive network in front of the original scattering load. Therefore, according to Bode–Fano theory, given the passive and causal nature of the cloak, inequality (2) expresses a local bound on 3D passive cloaking, independent of the employed matching network/cloaking technique and uniquely determined by the properties of the object to be cloaked (see also Supplement 1). It is also important to note that these physical bounds have been derived assuming a lossless scattering process (i.e., with zero absorption) to better identify and understand the ultimate cloaking limits directly imposed by passivity and causality. The presence of material losses would further deteriorate the performance of any cloaking device, as pointed out in, e.g., [12,14]. The derivation of more stringent bounds for a given level of absorption will be the subject of future investigations.

As an example, in Fig. 3(d) we visualize the calculated bound for the case of an impenetrable perfectly conducting sphere with radius $a = \lambda_c$. This example is particularly relevant for practical applications of cloaking technology, especially at RF and microwave frequencies, where several objects of interest, e.g., antennas, cellphones, and even the human body, have sizes in the order of a few free-space wavelengths. Similar to Fig. 2(d), the red thick line in Fig. 3(d) corresponds to the response of an optimal passive cloak, which indicates that a larger scattering suppression necessarily corresponds to a shrinking of the cloaking bandwidth [8–11]. Again, perfect cloaking is allowed only over a zero-measure frequency window, consistent with causality considerations [7]. The region beyond the physical bound may be accessed only by employing active or nonlinear cloaking designs [7,31–33] (however, only part of this region may be accessible, as causality limitations would still apply to active and nonlinear scatterers). The same bounds are also expected to apply to collections or arrays of cloaked objects, as studied, e.g., in [34].

On the same graph, we also visualize the performance of a typical transformation-optics (orange curve) and a single-layer plasmonic cloak (blue). Their SCS as a function of frequency is shown in Fig. 3(e), highlighting that, while for strong scattering suppression (more than 10 dB) transformation-optics cloaks provide a response close to the bound, if a larger level of scattering can be tolerated, there is room for improvement in terms of bandwidth. Wider bandwidths and larger scattering suppressions, corresponding to the empty portion of the realizable region in Fig. 3(d), may be reached by designing multi-layered Chebyshev-like passive cloaks, in direct analogy with the multi-layered planar cloaks presented in Fig. 2(e). An example of such a cloak is shown in Fig. 4(a) for the case of a moderately large dielectric sphere. As clearly seen in Fig. 4(a), while the designed cloak does not realize large scattering suppression at specific frequencies, a continuous scattering reduction of about 75% (6 dB) is achieved over a moderately broad bandwidth (about 20% of the central frequency). In strong similarity with the planar metasurface cloaks in Fig. 2(e), the scattering response around the cloaking frequency

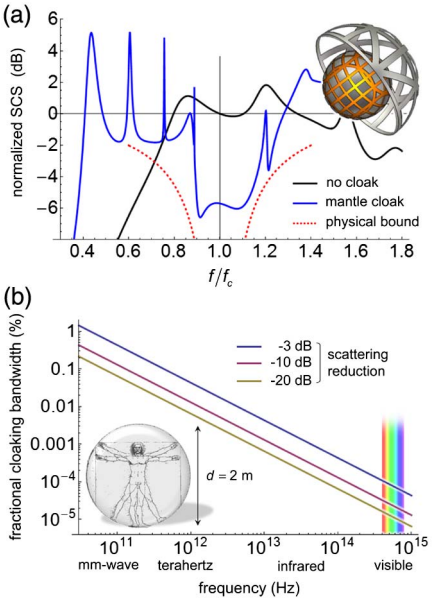

Fig. 4. Optimal passive cloaks. (a) Normalized scattering cross section of a moderately large dielectric sphere (black curve; diameter $d = \lambda_c/2$ at the cloaking wavelength λ_c, and relative permittivity $\epsilon = 5$) and of the same object surrounded by a Chebyshev-like cloak composed of two concentric metasurfaces (blue curve, details in Supplement 1). An illustration of the cloak is shown in the inset (only one hemisphere of the outer layer is shown). The physical bound is indicated by the dashed red line. (b) Scaling of the maximum fractional bandwidth, determined by our derived bounds, across the electromagnetic spectrum, from the millimeter-wave range to visible frequencies, for an impenetrable sphere of radius $a = 1$ m. The cloak aims at restoring the incident field distribution (in amplitude and phase) all around the obstacle. Three levels of scattering reduction are considered.

is characterized by in-band ripples and steep edges, which allows getting closer to the physical bound (red dashed line) by distributing the available scattering suppression over the allowed bandwidth. We also observe that the scattering reduction is obtained at the expense of significantly higher scattering over the rest of the spectrum, as also seen in the examples in Fig. 3(e), consistent with global cloaking bounds [19]. We expect that, by further increasing the number of concentric metasurfaces, and optimizing their reactance and separation, this approach may allow realizing optimal passive cloaks.

It is important to note that the derived bounds may be overcome if the object to be concealed is immersed in a medium with refractive index larger than unity (i.e., not free space), in which case the cloak may be made dispersionless, as proposed in [9], leading to a wider cloaking bandwidth. In general, the causality constraints on the scattered response are relaxed in media supporting wave speeds lower than the velocity of light [35]. For analogous reasons, acoustic cloaks are generally able to achieve significantly broader bandwidths than their electromagnetic counterparts [36], since they are not bound by limits on the background wave speed.

3. DISCUSSION

In the introduction, we asked ourselves whether it is at all possible to make a human-scale object invisible—or at least less

visible—over the entire visible spectrum, perhaps by using a cloaking device of arbitrarily large complexity. Our theory may provide a direct answer to this question: intuitively, if larger and larger scatterers are considered, more scattering harmonics are excited, which should all be minimized to attain invisibility at a given frequency, implying that the cloaking bounds are expected to become more and more stringent. This can be quantitatively predicted using Eq. (2), which, however, may not be convenient to use if the number N of contributions is large. Nevertheless, under some assumptions detailed in Supplement 1, Eq. (2) may be greatly simplified for large scatterers. In particular, for an impenetrable object of very large size, the derived bound can be approximated to

$$\frac{\mathrm{SCS}}{\pi a^2} \geq 2 \exp\left(-\frac{1}{B}\frac{2\pi}{k_0 a}\right). \tag{4}$$

If, for example, our goal were to cloak a human-scale object inside an impenetrable sphere of radius $a = 1$ m, Fig. 4(b) shows how the maximum fractional bandwidth of an optimal passive cloak would scale as a function of operating frequency based on this bound, from the millimeter-wave region, up to the visible range, for different levels of scattering reduction. For instance, a ten-fold suppression of SCS, at a central wavelength of $\lambda_c = 500$ nm (the color green), could be attained only within a fractional bandwidth $B = 0.00002\%$, which is much smaller than the typical bandwidth of LED light sources, and even of commercial diode lasers. Interestingly, a similar order of magnitude for the cloaking bandwidth was predicted in [15], based on very different arguments. More generally, we note that Eq. (4) is consistent with other bounds on cloaking bandwidth derived from causality considerations [8,13,15]. Our results ultimately confirm that broadband cloaking of macroscopic objects, in the sense of total scattering suppression (amplitude and phase recovery of an arbitrary impinging wave), is impossible with linear and passive cloaks of arbitrary complexity. These hard bounds on free-space cloaking may be overcome only by using active and nonlinear designs [7,31–33] or by relaxing the requirements on the phase scattering pattern [2,37] and/or the omnidirectionality of the invisibility phenomenon [16–18].

In conclusion, our findings address the current challenges in realizing reasonably broadband invisibility cloaks and provide quantitative tools to assess the realistic applicability of cloaking technologies in practical scenarios. Ten years after the first pioneering works on invisibility cloaks, our results solidify the claim that broadband cloaking of electrically large objects is practically impossible and provide, for the first time, to the best of our knowledge, a quantitative assessment of the limits of arbitrary passive cloaks. We believe this represents an important result for the science of cloaking, suggesting that new concepts and designs, including opening to the field of nonlinear and active metamaterials, are necessary to move forward in the quest for invisibility.

Funding. National Science Foundation (NSF) (ECCS-0953311); Air Force Office of Scientific Research (AFOSR) (FA9550-13-1-0204); Defense Threat Reduction Agency (DTRA) (HDTRA1-12-1-0022).

See Supplement 1 for supporting content.

REFERENCES

1. N. Engheta and R. W. Ziolkowski, eds., *Metamaterials: Physics and Engineering Explorations* (Wiley-IEEE, 2006).
2. U. Leonhardt, "Optical conformal mapping," Science **312**, 1777–1780 (2006).
3. J. B. Pendry, D. Schurig, and D. R. Smith, "Controlling electromagnetic fields," Science **312**, 1780–1782 (2006).
4. A. Alù and N. Engheta, "Achieving transparency with plasmonic and metamaterial coatings," Phys. Rev. E **72**, 016623 (2005).
5. A. Alù, "Mantle cloak: invisibility induced by a surface," Phys. Rev. B **80**, 245115 (2009).
6. R. Fleury, F. Monticone, and A. Alù, "Invisibility and cloaking: origins, present, and future perspectives," Phys. Rev. Appl. **4**, 037001 (2015).
7. D. A. B. Miller, "On perfect cloaking," Opt. Express **14**, 12457–12466 (2006).
8. H. Chen, Z. Liang, P. Yao, X. Jiang, H. Ma, and C. T. Chan, "Extending the bandwidth of electromagnetic cloaks," Phys. Rev. B **76**, 241104(R) (2007).
9. A. Alù and N. Engheta, "Effects of size and frequency dispersion in plasmonic cloaking," Phys. Rev. E **78**, 045602 (2008).
10. B. Zhang, B.-I. Wu, H. Chen, and J. A. Kong, "Rainbow and blueshift effect of a dispersive spherical invisibility cloak impinged on by a nonmonochromatic plane wave," Phys. Rev. Lett. **101**, 063902 (2008).
11. E. Kallos, C. Argyropoulos, Y. Hao, and A. Alù, "Comparison of frequency responses of cloaking devices under nonmonochromatic illumination," Phys. Rev. B **84**, 045102 (2011).
12. H. Hashemi, B. Zhang, J. Joannopoulos, and S. Johnson, "Delay-bandwidth and delay-loss limitations for cloaking of large objects," Phys. Rev. Lett. **104**, 253903 (2010).
13. H. Hashemi, C.-W. Qiu, A. P. McCauley, J. D. Joannopoulos, and S. G. Johnson, "Diameter-bandwidth product limitation of isolated-object cloaking," Phys. Rev. A **86**, 013804 (2012).
14. H. Hashemi, A. Oskooi, J. D. Joannopoulos, and S. G. Johnson, "General scaling limitations of ground-plane and isolated-object cloaks," Phys. Rev. A **84**, 023815 (2011).
15. C. Craeye and A. Bhattacharya, "Rule of thumb for cloaking bandwidth based on a wave-packet argument," IEEE Trans. Antennas Propag. **60**, 3516–3520 (2012).
16. A. Plakhov and V. Roshchina, "Invisibility in billiards," Nonlinearity **24**, 847–854 (2011).
17. H. Chen, B. Zheng, L. Shen, H. Wang, X. Zhang, N. I. Zheludev, and B. Zhang, "Ray-optics cloaking devices for large objects in incoherent natural light," Nat. Commun. **4**, 2652 (2013).
18. J. S. Choi and J. C. Howell, "Paraxial ray optics cloaking," Opt. Express **22**, 29465–29478 (2014).
19. F. Monticone and A. Alù, "Do cloaked objects really scatter less?" Phys. Rev. X **3**, 041005 (2013).
20. F. Monticone and A. Alù, "Physical bounds on electromagnetic invisibility and the potential of superconducting cloaks," Photon. Nanostruct. **12**, 330–339 (2014).
21. H. Bode, *Network Analysis and Feedback Amplifier Design* (David Van Nostrand, 1945).
22. R. M. Fano, "Theoretical limitations on the broadband matching of arbitrary impedances," J. Franklin Inst. **249**, 57–83 (1950).
23. M. Gustafsson and S. Nordebo, "Bandwidth, Q factor, and resonance models of antennas," Prog. Electromagn. Res. **62**, 1–20 (2006).
24. P. Alitalo and S. A. Tretyakov, "Broadband electromagnetic cloaking realized with transmission-line and waveguiding structures," Proc. IEEE **99**, 1646–1659 (2011).
25. R. Schittny, M. Kadic, T. Bückmann, and M. Wegener, "Invisibility cloaking in a diffusive light scattering medium," Science **345**, 427–429 (2014).
26. J. Li and J. B. Pendry, "Hiding under the carpet: a new strategy for cloaking," Phys. Rev. Lett. **101**, 203901 (2008).
27. D. M. Pozar, *Microwave Engineering*, 3rd ed. (Wiley, 2011).
28. C. F. Bohren and D. R. Huffman, *Absorption and Scattering of Light by Small Particles* (Wiley, 1983).
29. N. Engheta, A. Salandrino, and A. Alù, "Circuit elements at optical frequencies: nanoinductors, nanocapacitors, and nanoresistors," Phys. Rev. Lett. **95**, 095504 (2005).
30. M. Staffaroni, J. Conway, S. Vedantam, J. Tang, and E. Yablonovitch, "Circuit analysis in metal-optics," Photon. Nanostruct. **10**, 166–176 (2012).

31. F. Guevara Vasquez, G. W. Milton, and D. Onofrei, "Broadband exterior cloaking," Opt. Express **17**, 14800–14805 (2009).
32. P.-Y. Chen, C. Argyropoulos, and A. Alù, "Broadening the cloaking bandwidth with non-Foster metasurfaces," Phys. Rev. Lett. **111**, 233001 (2013).
33. D. L. Sounas, R. Fleury, and A. Alù, "Unidirectional cloaking based on metasurfaces with balanced loss and gain," Phys. Rev. Appl. **4**, 014005 (2015).
34. M. Farhat, P.-Y. Chen, S. Guenneau, S. Enoch, R. McPhedran, C. Rockstuhl, and F. Lederer, "Understanding the functionality of an array of invisibility cloaks," Phys. Rev. B **84**, 235105 (2011).
35. A. N. Norris, "Acoustic integrated extinction," Proc. R. Soc. A **471**, 20150008 (2015).
36. A. N. Norris, "Acoustic cloaking," Acoust. Today **11**(1), 38–46 (2015).
37. U. Leonhardt and T. Tyc, "Broadband invisibility by non-Euclidean cloaking," Science **323**, 110–112 (2009).